Experimental Investigations on Reinforced Concrete Slabs Subjected to Impact Loading

T. Uchida, H. Tsubota, T. Yamada
Kajima Institute of Construction Technology, 19-1 Tobitakyu 2-chome, Chofu-shi, Tokyo 182, Japan

Abstract

Impact loading tests of reinforced concrete slabs with extensive test parameters were performed. An improved impact loading method using a freely falling mass, which enables to control peak values and durations of contact loads, was developed. From the test results, the overall response behavior of slabs under impact loading became clear. Especially, a quantitative comparison of the capacity of energy absorption between the slabs under static and impact loading was performed. By comparing test results with a simplified analytical method with single D.O.F. system and a nonlinear finite element analysis, the applicability of both analytical methods was evaluated.

1. Introduction

In designing nuclear power plant structures, it is required to ensure their structural safety against impact loads induced by aircraft crash or other missiles. The purpose of this experimental investigation is to clarify the behavior of reinforced concrete slabs subjected to impact loading and to establish a rational design method through the verification of a simplified analysis with single D.O.F. system and a nonlinear finite element analysis.

2. Development of Testing Method

The impact load was applied to the specimen by means of a freely falling mass. It is very difficult, in general, to control peak values(Fmax) and durations(td) of impact loads by this method. To solve this problem, a buffer(rubber pad) was installed to the specimen just at the contact point of falling mass, with the aim of controling Fmax with the velocity(V) of falling mass and td with the thickness of rubber pad(tr) independently. To confirm this control method, a preliminary test by using specimens of steel plate was performed. As the result, td was mainly affected by tr and kept almost constant value regardless with the change of V and the relationship between Fmax and V was also grasped quantitatively (Fig.1). Consequently, it was found that the proposed method was applicable to the impact loading test of reinforced concrete slabs. Fig.2 shows the arrangement of impact test rig. To prevent the mass from dropping again on the surface of specimen, a photoelectronic switch which perceives the passing of the falling mass was installed just above the contact point. This switch was interlocked with two electromagnets attached on both sides of the mass through a timer and the rebounded mass was attracted to steel guide by the magnetic attraction. The impact load, reaction forces, displacement of specimen and strain of reinforcing bars were measured. Measuring instruments whose response frequency is more than 20kHz were used. In order to

provide a trigger which urges automatic data recording, an on-off signal of laser beam intercepted by falling mass, was utilized.

3. Test Specimen and Parameters

About 30 specimens of reinforced concrete slabs, including specimens for static loading test, were tested. The specimens are square slabs with 1.8m side length and supported at the four corner points with 1.5m span length. The main parameters considered in this experiment are profile of impact load, slab thickness, bending and shear reinforcement ratio and mixture ratio of steel fiber. The detail of parameters is shown in Table 1.

4. Test Results

The main test results are summarized in Table 1 and, for example, some time history curves of measured data are shown in Fig.3. Fig.4 shows the difference of cracking patterns between the slabs under static and impact loading. Under static loading, in general, cracks occur only on the rear face of the specimen and progress on transverse directions along yield lines. At first, the bending deformation is dominant under static loading and after yielding of bending rebars, the specimen reaches failure with local punching shear mode. Under impact loading, on the other hand, the occurrence of yield lines becomes indistinct and circular cracks on the front face and diagonal cracks on the rear face occur due to the vibration of slab and the propagation of shock wave. Finally, most specimens indicated the punching shear failure mode as shown in Photo.1. It became clear that the additional shear reinforcement or mixture of steel fiber is very effective to decrease the formation of cracks under impact loading.

The load-displacement curves obtained from impact loading tests are compared with the static one in Fig.5. As shown in this figure, the discrepancy between both curves is remarkable. However, the load-displacement curve under impact loading tends to converge to the static one as the loading rate decreases. The absorbed energy under static and impact loading (Es and Ed) was calculated by integrating the enclosed area of both load-displacement curves up to the maximum response displacement. The ratio of Ed to Es of all specimens are indicated in Fig.6, using td/T (T: the 1st natural period of the slab) as parameters. The energy absorbed in slabs under impact loading increases in proportion to the loading rate and reaches up to almost two times the static one. In case of slabs with steel fiber mixture this tendency becomes more remarkable and Ed is more than four times as large as Es. This large discrepancy of the energy absorption between static and impact loading may be caused by difference of deformation modes, that is bending mode under static loading and punching shear mode under impact loading.

5. Comparison with Analytical Results

Test results were compared with following two analytical methods:

(1) Simplified Analytical Method [1] : In this analytical method, the specimen was idealized as a single degree of freedom system with one equivalent mass and a bilinear resistance function, evaluated from the static test result. On the other hand, the obtained load-time function was idealized as a triangular pulse load with same amount of impulse. The comparison of calculated and measured maximum displacement is shown in Fig.7. The calculated values are smaller than test results, and this simplified analytical method gives a conservative evaluation. Some specimens show large discrepancy between analytical and measured results and this discrepancy may be due to the fault of the idealization of specimen. For such specimens, their equivalent mass and resistance function must be

reevaluated according to the punching shear mode.

(2)Nonlinear Finite Element Analysis [2] : The following assumptions were employed.

1) The reinforced concrete slab was approximated as an assemblage of flat quadrilateral elements with the layer approach applying the classical Kirchhoff's hypothesis. Each flat quadrilateral element was composed of four triangular elements, derived from combining a linear curvature bending element developed by Clough and Fellipa [3] with a constant strain membrane element.
2) The stress-strain relationship of the reinforcing bar was assumed to be a bilinear type. The concrete was assumed to have two plasticities, plasticity in compression and cracking in tension. The plasticity was based on the Drucker-Prager's criterion, the normality flow rule and isotropic hardening. The cracking was defined by the maximum principal stress criterion.
3) When stress exceeded the yield point or cracking of concrete occurred, the unbalanced force was reevaluated and released in the next calculation step.
4) In dynamic analysis, the rotatinal inertia was ignored and the implicit integration method was used for time integration.

The calculated time history of the displacement at the center of slab is shown in Fig.8, comparing with the test result. When the loading rate is small, both the calculated maximum displacement and it's occurrence time are very close to those obtained experimentally. As the loading rate increases, however, a little difference arises between calculated and measured result. In Fig.9, the final cracking pattern obtained from analysis is shown in comparison with the test result. It is confirmed that not only the bending cracks on rear face but also the circular cracks on front face, which are peculiar to the impact loading test, can be predicted by the proposed analytical method.

6. Conclusion

Main conclusions obtained from this experimental investigations are as follows;

(1) The characteristics of the cracking formation, deformation mode and failure pattern of reinforced concrete slabs subjected to impact loading were clarified.
(2) A quantitative grasp of the capacity of energy absorption of slabs under static and impact loading were performed. Especially, it became clear that the impactive energy absorption increases remarkably by mixing steel fiber.
(3) A simplified analytical method with single D.O.F. system gave a conservative evaluation.
(4) The proposed finite element analysis method was able to predict the overall behavior of reinforced concrete slabs subjected to impact loading.

Acknowledgement

The authors wish to express their gratitude to Dr. Kiyoshi Muto for pertinent guidances given to this research work.

References

[1] BIGGS,J.M.,"Introduction to Structural Dynamics", McGRAW HILL, 1964.
[2] MORIKAWA,H.,"Nonlinear Analysis of Reinforced Concrete Cylindrical Shell Subjected to Internal Pressure and/or Thermal Loads with Seismic Loads(in Japanese)", Proceedings of JCI Colloquium on Finite Element Analysis of RC Structures, Dec. 12, 1984.
[3] CLOUGH,R.W. and FELLIPA,C.A.,"A Refined Quadrilateral Element for Analysis of Plate Bending", AFTDL-TR-68-150.

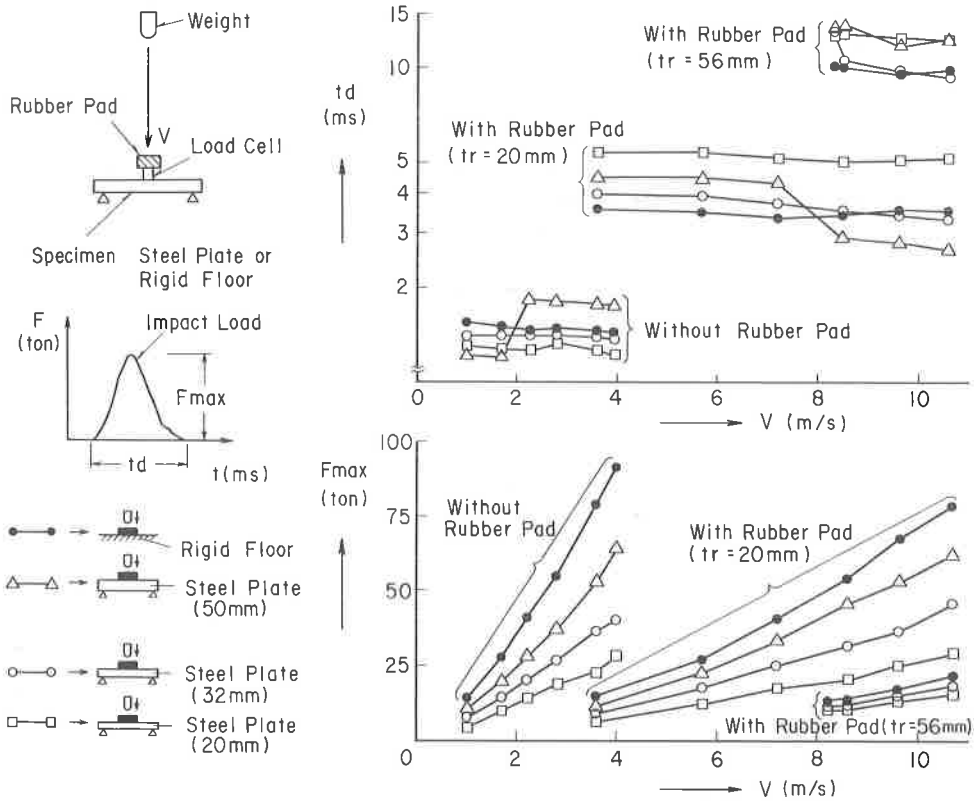

Fig. 1 Results of Preliminary Test

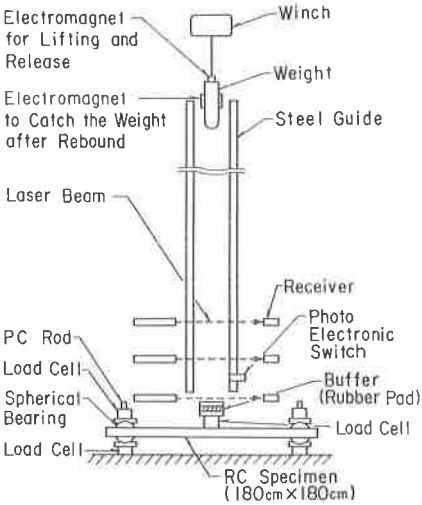

Fig.2 Arrangement of Impact Test Rig

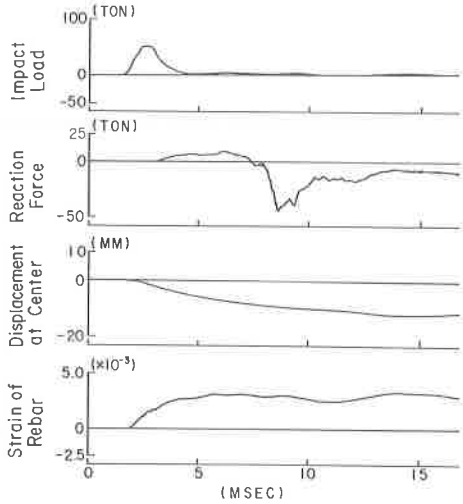

Fig. 3 Time History Curves of Measured Data

Table 1 Test Parameters and Results

Specimen	Thickness of Slab (mm)	Reinforcement Ratio		Steel Fiber Mix. Ratio (%)	Impact Loading Test			Static Test	
		Bending (%)	Shear (%)		Fmax. (ton)	td (msec)	Max. Disp. (mm)	Ult. Load (ton)	Ult. Disp. (mm)
A3	80.0	0.3	—	—	32.1	4.1	34.8	5.7	71.8
B3-1	120.0	0.3	—	—	59.4	1.1	4.5	10.6	62.5
B3-2					27.0	3.4	7.5		
B3-3					51.9	2.6	11.6		
B3-4					19.0	8.5	12.8		
B3-5					83.6	1.4	8.4		
B3-6					15.9	5.3	6.9		
B6	120.0	0.6	—	—	42.0	3.2	13.0	15.5	29.4
B9	120.0	0.9	—	—	37.0	3.3	11.7	19.5	27.3
B12	120.0	1.2	—	—	50.6	3.5	13.9	23.5	19.2
BSF3-1	120.0	0.3	—	2.0	77.2	1.3	5.1	12.3	68.9
BSF3-2					52.0	2.9	9.6		
BSF3-3					22.4	7.5	8.7		
BSF3-4					67.7	1.1	3.9		
BSF3-5					18.0	4.0	3.9		
BQ12-6	120.0	0.3	0.6	—	44.4	3.4	12.9	25.1	38.8
BQ12-12			1.2		44.9	3.5	12.7	26.0	34.9
BR3	120.0	0.3	—	—	52.8	2.6	17.1	8.8	57.2
C3	200.0	0.3	—	—	63.3	2.3	5.4	24.4	24.3

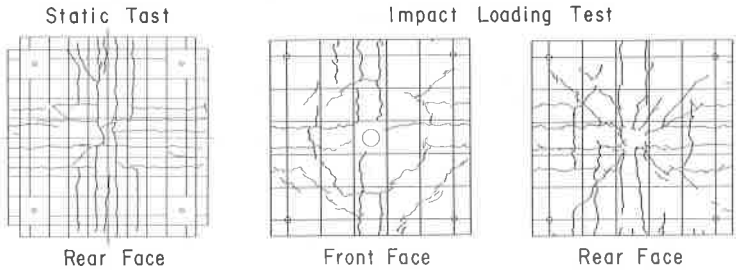

Fig. 4 Observed Final Cracking Pattern

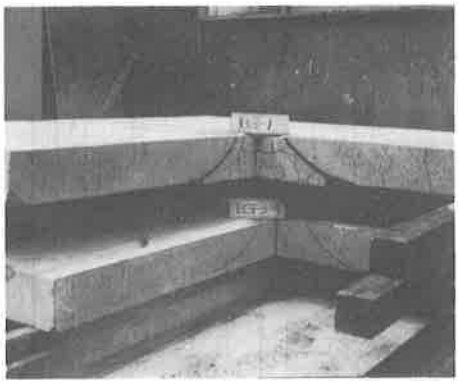

Photo. 1 Punching Shear Failure Mode

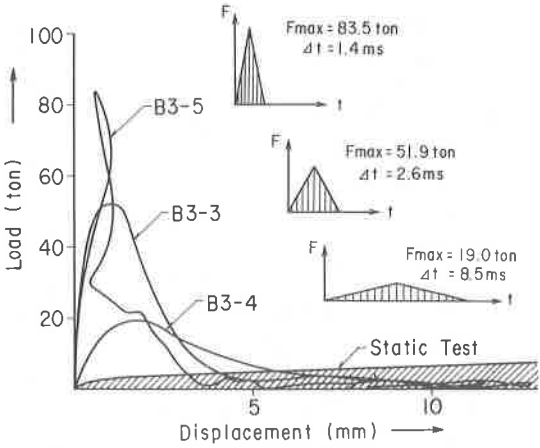

Fig. 5 Load-Displacement Curves

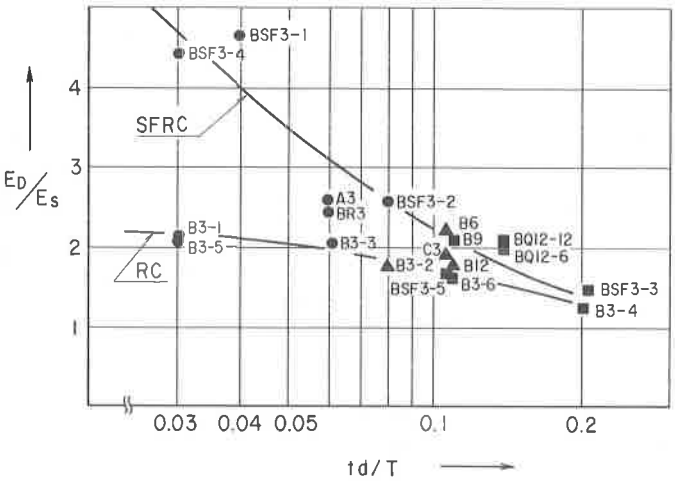

Fig. 6 Comparison of Absorbed Energy under Static and Impact Loading

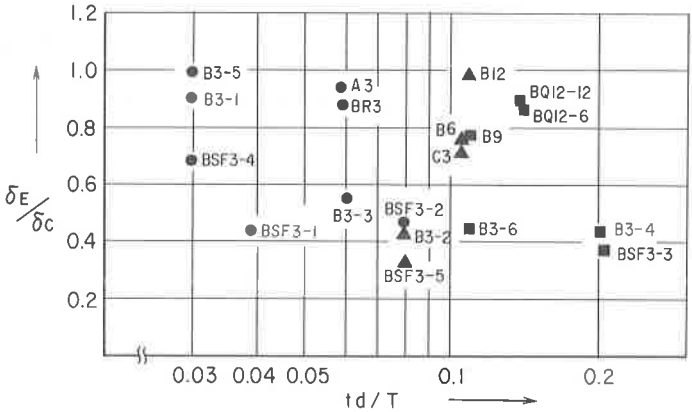

Fig. 7 Comparison of Calculated and Measured Maximum Displacement

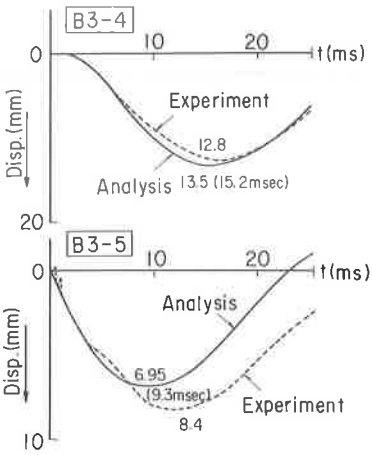

Fig. 8 Time History of Displacement

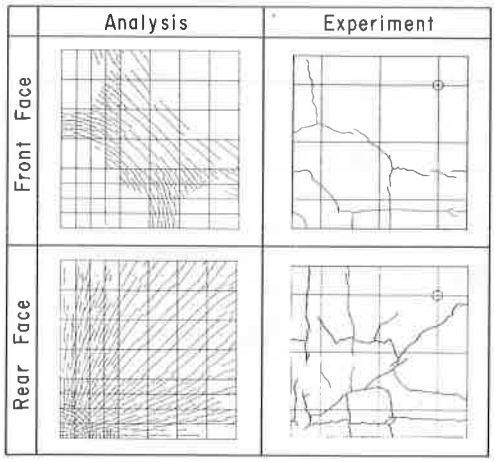

Fig. 9 Final Cracking Pattern